AIP Journal of Applied Physics

Influence of particle-matrix interface, temperature, and agglomeration on heat conduction in dispersions

A. Behrang, M. Grmela, C. Dubois, S. Turenne, and P. G. Lafleur

Citation: Journal of Applied Physics **114**, 014305 (2013); doi: 10.1063/1.4812734
View online: http://dx.doi.org/10.1063/1.4812734
View Table of Contents: http://scitation.aip.org/content/aip/journal/jap/114/1?ver=pdfcov
Published by the AIP Publishing

Influence of particle-matrix interface, temperature, and agglomeration on heat conduction in dispersions

A. Behrang,[1] M. Grmela,[2,a)] C. Dubois,[2] S. Turenne,[1] and P. G. Lafleur[2]
[1]*Department of Mechanical Engineering, École Polytechnique de Montreal, Montréal, Quebec H3C 3A7, Canada*
[2]*Department of Chemical Engineering, École Polytechnique de Montreal, Montréal, Quebec H3C 3A7, Canada*

(Received 8 April 2013; accepted 17 June 2013; published online 3 July 2013)

A combination of the effective medium and the phonon approaches is used to investigate heat conduction in heterogeneous media composed of a homogeneous matrix in which spherical particles of micro and nanosizes are dispersed. In particular, we explore the effect of different types of scattering on the particle-matrix interface, temperature dependence of the effective heat conduction coefficient, and the effect of various degrees of agglomeration of the particles. Predictions calculated explicitly for Si nanoparticles dispersed in Ge matrix agree with available Monte Carlo simulations. Our predictions show that the higher is the temperature the lower is the heat conductivity and the smaller is the influence of the details of the particle-matrix interactions. As for the influence of the agglomeration, we predict both decrease and increase of the heat conduction depending on the degree of the agglomeration. © *2013 AIP Publishing LLC*.
[http://dx.doi.org/10.1063/1.4812734]

I. INTRODUCTION

We investigate heat conduction in two component heterogeneous media. One component is a homogeneous matrix in which the second component is dispersed in the form of spherical particles. If the dimension of the spheres is larger than the phonon mean free path then the heat conduction is well described by the classical Fourier theory. Due to the heterogeneity, its application results in a complex system of partial differential equations and boundary conditions. It has been shown in Refs. 1 and 2 that the system can be simplified by appropriately homogenizing the heterogeneous medium. The resulting homogeneous medium is called an effective medium and the approach to investigate in this way heat conduction in heterogeneous media is called an effective medium approach (this approach has been introduced first in the context of electric conductivity in Ref. 3). The heat conductivity k_{eff} of the effective medium that arises in Ref. 2 is given by

$$k_{eff} = k_m \frac{2k_m + (1+2\alpha)k_p + 2\phi[(1-\alpha)k_p - k_m]}{2k_m + (1+2\alpha)k_p - \phi[(1-\alpha)k_p - k_m]}. \quad (1)$$

The symbol ϕ stands for the volume fraction of the suspended particles, and k_m and k_p for the heat conductivity coefficient of the matrix and the suspended particle. The influence of the particle-matrix interface is expressed in Eq. (1) in the dimensionless parameter $\alpha = \frac{a_K}{a_p}$, where a_p is the radius of the spherical particle and $a_K = Rk_m$ is the thickness of the matrix-filled layer surrounding the particle in which the same temperature drop occurs as that at the interface. The coefficient R is called a thermal boundary resistance coefficient. If $a_K = 0$, and thus $\alpha = 0$ then the interface is called a perfect interface.

If, on the other hand, the dimension of the spheres is smaller than the phonon mean free path then the heat conduction has to be approached with the Boltzmann-Peierls theory in which heat is seen as a gas of phonons (see Refs. 4–7). The mathematical formulation consists of the Boltzmann-type equation governing the time evolution of the one-phonon distribution function in the heterogeneous medium under consideration. We shall not take this route.

In this paper, we follow a third route, introduced originally in Refs. 8 and 9, which is a hybrid of the previous two. The starting point is the expression Eq. (1) for the heat conductivity of an effective homogeneous medium. The phonon viewpoint of heat is introduced into Eq. (1) in expressions for the coefficients k_m, k_p, and α that arises in the Boltzmann-Peierls phonon theory. Our contribution consists of (i) a new consideration of the matrix-particle interface (Sec. II), (ii) an explicit investigation of the temperature dependence of k_{eff} that follows from its phonon representation (Sec. III), and (iii) an investigation of the influence of various degrees of agglomeration of the dispersed particles (Sec. IV). Our motivation and a potential domain of application is an attempt to increase the efficiency of thermoelectric devices measured by $S^2\sigma T/k$, where S is the Seebeck coefficient, σ is the electric conductivity, T is the absolute temperature, and k is the thermal conductivity.[10,11] In this paper, we are addressing only the heat conductivity which, according to experimental observations,[12–17] plays a dominant role in the increase of the thermoelectric efficiency.

II. PHONON REPRESENTATION OF THE EFFECTIVE FOURIER HEAT CONDUCTION

We recall first the phonon representation of Eq. (1) derived in Refs. 8 and 9. The Boltzmann-Peierls phonon theory applied to a homogeneous medium leads to the following expression for the heat conductivity coefficient k:

a)Electronic mail: miroslav.grmela@polymtl.ca

$$k = \frac{1}{3}\int C(\omega)v(\omega)\Lambda(\omega)d\omega \approx \frac{1}{3}Cv\Lambda, \tag{2}$$

where C is the volumetric specific heat per unit frequency at the frequency ω, v is the phonon group velocity, and Λ is the phonon mean free path.

In the absence of particles the phonons experience inside the matrix phonon-phonon and phonon-impurities interactions. The average distance between two subsequent collisions is the (bulk) mean free path denoted $\Lambda_{b,m}$. Similarly, $\Lambda_{b,p}$ is the (bulk) mean free path inside the particles. In the presence of both the matrix and the particles, the phonons interact (collide) in additions also with the matrix-particle interface. These interactions are of two types: (i) *collisions* in which the incoming and outcoming phonons remain on the same side of the interface and (ii) *transmission interactions* in which phonons pass the interface. Each of these interactions can be then again of two types: (a) *diffuse* in which the direction of the phonon after the interaction is independent of the direction of the impacting phonons, and (b) *specular* in which the incident angle influences the outcome of the interaction. As to whether the interactions are diffuse or specular depends on details of the physics of the interface. In general, we can anticipate that the more complex is the interface the more diffuse is the scattering. For example, the specular interactions are expected to play an important role in very low temperatures when thermal motion is week and the interface is microscopically smooth.

A. Diffuse scattering mechanism

In the investigation reported in Refs. 8 and 9 all phonon-interface scatterings are assumed to be diffuse. For the collision interactions, Minnich and Chen[8] use $\Lambda_{coll,m} = \frac{4a_p}{3\phi}$ and $\Lambda_{coll,p} = 2a_p$, where $\Lambda_{coll,m}$ denotes the collision mean free path in the matrix and $\Lambda_{coll,p}$ in the particles.

The transmission interaction is taken into account in Refs. 8 and 9 in the coefficient α appearing in Eq. (1). The specific expression for α used there is the one introduced in Ref. 18 by using emitted temperature approximation: $\alpha = \frac{Rk_m}{a_p}$ with $R = 4\left(\frac{C_m v_m + C_p v_p}{C_m v_m C_p v_p}\right)$.

Finally, in order to find the mean free path corresponding to both types of interactions (i.e., those inside the bulk and with the interface) It is assumed in Refs. 8 and 9 that both of these interactions are independent and the mean free path is given by the empirical Matthiessen rule

$$\frac{1}{\Lambda_j} = \frac{1}{\Lambda_{b,j}} + \frac{1}{\Lambda_{coll,j}} \quad j = m,p. \tag{3}$$

The subscripts p and m denote "particle" and "matrix," respectively, b stands for "bulk," and *coll* for "collisions." Alternatively, the expression Eq. (3) is also written in the form

$$\Lambda_j = F_j\Lambda_{b,j}, \quad i = p,m, \tag{4}$$

which defines the scaling factor F_j by requiring that Eqs. (4) and (3) are equivalent.

By inserting the above expressions into Eq. (1), one obtains the phonon representation of Eq. (1) derived in Refs. 8 and 9.

B. Diffuse and specular scattering mechanisms

We now proceed to present our alternative approach. Our aim is to pay more attention to the phonon-interface interactions. In particular, our intention is to explore, in addition to the contribution to k_{eff} from diffuse interactions, also the contribution brought about by specular interactions.

We assume that the effective heat conductivity k_{eff} is a linear combination of $k_{eff}^{(s)}$ (corresponding to the case when all phonon-interface interactions are specular) and $k_{eff}^{(d)}$ (corresponding to the case when all phonon-interface interactions are diffuse)

$$k_{eff} = sk_{eff}^{(s)} + (1-s)k_{eff}^{(d)}, \tag{5}$$

where s is a phenomenological parameter, $0 \le s \le 1$, having the physical interpretation of the probability of the specular scattering of phonons on the particle-matrix interface. Its value is found by comparing predictions with results of experimental observations. We shall see below that such comparison shows that the diffuse interactions play a dominant role but a small value of s slightly improves the agreement of predictions with results of experimental observations.

We continue by expressing both $k_{eff}^{(s)}$ and $k_{eff}^{(d)}$ in the form (2) with the mean free paths $\Lambda_j^{(i)}; i = s,d \quad j = m,p$.

To combine the interactions, we again use the Mathiessen rule. Since we consider now also phonon-interface transmission interactions, we replace Eq. (3) with

$$\frac{1}{\Lambda_j^{(i)}} = \frac{1}{\Lambda_{b,j}^{(i)}} + \frac{1}{\Lambda_{coll,j}^{(i)}} + \frac{1}{\Lambda_{TBR,j}^{(i)}}, \quad i = s,d \quad j = m,p. \tag{6}$$

The last term on the right hand side of Eq. (6) is the contribution from the transmission interactions, Λ_{TBR} is the *thermal boundary resistance* mean free path (a ratio between the transmission length and the number of transmissions).

Now, we proceed to specify the mean free paths in diffuse and specular phonon-interface scatterings.

For diffuse collisions and for particles, we use $\Lambda_{coll,p}^{(d)} = \frac{3a_p}{4}$ proposed in Ref. 19. For the matrix, we keep the same $\Lambda_{coll,m}^{(d)}$ as in Minnich and Chen[8] analysis (i.e., $\Lambda_{coll,m} = \frac{4a_p}{3\phi}$). For the specular collisions we make the same choice as for the diffuse collisions except that, following Ref. 20, we replace the particle radius a_p with an effective particle radius $a_p^{(s)} = a_p\frac{1+s}{1-s}$, where s is the parameter appearing in Eq. (5). This means that $\Lambda_{coll,m}^{(s)} = \frac{4a_p^{(s)}}{3\phi}$ and $\Lambda_{coll,p}^{(s)} = \frac{3a_p^{(s)}}{4}$. We note that for the pure specular collisions (i.e., the case when $s = 1$) $(\Lambda_{coll,m}^{(s)})^{-1} = (\Lambda_{coll,p}^{(s)})^{-1} = 0$, and consequently (see Eq. (6)) collisions do not contribute to the effective mean free path.

Now we turn to the transmission scattering. We recall that in Refs. 8 and 9 these interactions are taken into

account in the parameter α appearing in Eq. (1). We take them into account, on the other hand, in the third term on the right hand side of Eq. (6). We thus put $\alpha = 0$ in Eq. (1) and focus our attention on Λ_{TBR}. We follow closely Refs. 18 and 20 where this investigation is made in a somewhat different context (superlattices). Based on the equivalent equilibrium temperature of phonons on each side of the interface (see Sec. II B in Ref. 18 and Sec. II G in Ref. 20) we arrive at

$$\Lambda^{(i)}_{TBR,p} = 0 \quad for \;\; i = s,d,$$

$$\Lambda^{(d)}_{TBR,m} = \frac{a_p t^{(d)}_{mp}}{\phi\left[1 - \frac{1}{2}(t^{(d)}_{mp} + t^{(d)}_{pm})\right]},$$

$$\Lambda^{(s)}_{TBR,m} = \frac{2a_p \int_0^{\mu_{crit}} t^{(s)}_{mp}(\mu_m)\mu_m d\mu_m}{\phi\left[1 - \int_0^{\mu_{crit}} t^{(s)}_{mp}(\mu_m)\mu_m d\mu_m - \int_0^{\mu_{crit}} t^{(s)}_{pm}(\mu_p)\mu_p d\mu_p\right]}. \tag{7}$$

The symbol $t^{(d)}_{jl}$ denotes the probabilities of transmission from side "j" to side "l" in the diffuse scattering. They are given by $t^{(d)}_{jl} = \frac{C_l v_l}{C_j v_j + C_l v_l}$, $j,l = p,m$; $j \neq l$. The symbol $t^{(s)}_{jl}$ denotes the probabilities of transmission from side "j" to side "l" in the specular scattering. They are given by $t^{(s)}_{pm} = \frac{4\rho_p v_p \rho_m v_m \mu_p \mu_m}{(\rho_p v_p \mu_p + \rho_m v_m \mu_m)^2}$ and $t^{(s)}_{mp} = \frac{C_p v_p^3}{C_m v_m^3} t^{(s)}_{pm}$, where $\mu_m = \cos\theta_m$ and $\mu_p = \cos\theta_p$ are related by Snell's law $\frac{\sin\theta_m}{v_m} = \frac{\sin\theta_p}{v_p}$, the critical angle θ_{crit} appearing in the formula for $F^{(s)}_m$ is given by $\theta_{crit} = \arcsin\frac{v_p}{v_m}$ if $v_m > v_p$ and $= 0$ if $v_m < v_p$ for phonon transmission from particle to matrix. In the opposite case for phonon transmission from matrix to particle, $\theta_{crit} = \arcsin\frac{v_m}{v_p}$ if $v_p > v_m$ and $= 0$ if $v_p < v_m$. By $a^{(s)}_p = a_p\frac{1+s}{1-s}$, we denote the effective particle radius, ρ_m and ρ_p denote the mass density of the matrix and the particle, respectively. The expressions for the probabilities of specular transmission are valid when the incident angle is smaller than a critical angle θ_c. Otherwise, there is no transmission of phonons.[18]

With the expressions for the mean free paths introduced above, the formula Eq. (1) takes the form

$$k^{(i)}_{eff} = \frac{1}{3}C_m v_m \Lambda_{b,m} F^{(i)}_m \frac{\frac{2}{3}C_m v_m \Lambda_{b,m} F^{(i)}_m + \frac{1}{3}C_p v_p \Lambda_{b,p} F^{(i,1)}_p + 2\phi\left(\frac{1}{3}C_p v_p \Lambda_{b,p} F^{(i,2)}_p - \frac{1}{3}C_m v_m \Lambda_{b,m} F^{(i)}_m\right)}{\frac{2}{3}C_m v_m \Lambda_{b,m} F^{(i)}_m + \frac{1}{3}C_p v_p \Lambda_{b,p} F^{(i,1)}_p - \phi\left(\frac{1}{3}C_p v_p \Lambda_{b,p} F^{(i,2)}_p - \frac{1}{3}C_m v_m \Lambda_{b,m} F^{(i)}_m\right)}, \quad i = s,d, \tag{8}$$

where F, scaling coefficients related to the mean free paths Λ by the relation (4), are given by

$$F^{(i,1)}_p = F^{(i,2)}_p; \;\; i = s,d, \quad F^{(d)}_m = \frac{4\frac{a_p}{\Lambda_{b,m}} t^{(d)}_{mp}}{4\frac{a_p}{\Lambda_{b,m}} t^{(d)}_{mp} + \phi[t^{(d)}_{mp} - 2t^{(d)}_{pm} + 4]},$$

$$F^{(s)}_m = \frac{4\frac{a_p}{\Lambda_{b,m}} \int_0^{\mu_{crit}} t^{(s)}_{mp}(\mu_m)\mu_m d\mu_m}{4\frac{a_p}{\Lambda_{b,m}} \int_0^{\mu_{crit}} t^{(s)}_{mp}(\mu_m)\mu_m d\mu_m + \phi\left[2\left(1 - \int_0^{\mu_{crit}} t^{(s)}_{pm}(\mu_m)\mu_m d\mu_m\right) + \int_0^{\mu_{crit}} t^{(s)}_{mp}(\mu_p)\mu_p d\mu_p \left(\frac{3a_p}{a^{(s)}_p} - 2\right)\right]}, \tag{9}$$

$$F^{(d)}_p = \frac{3\frac{a_p}{\Lambda_{b,p}}}{3\frac{a_p}{\Lambda_{b,p}} + 4}, \quad F^{(s)}_p = 1.$$

The formulas derived in Refs. 8 and 9 are a particular case of Eqs. (5) and (8) corresponding to no specular scattering (i.e., $s = 0$, and thus also $F^{(s)}_m = 0, F^{(s,1)}_p = 0, F^{(s,2)}_p = 0$) and $F^{(d)}_m = \frac{4a_p}{\Lambda_{b,m}}(\frac{4a_p}{\Lambda_{b,m}} + 3\phi)^{-1}$, $F^{(d,1)}_p = (\frac{2a_p}{\Lambda_{b,p}})(1 + 2\alpha(\phi, a_p))(\frac{2a_p}{\Lambda_{b,p}} + 1)^{-1}$, $F^{(d,2)}_p = (\frac{2a_p}{\Lambda_{b,p}})(1 - \alpha(\phi, a_p))(\frac{2a_p}{\Lambda_{b,p}} + 1)^{-1}$, together with $\alpha = a_K/a_p$ with the thermal boundary resistance coefficient (i.e., R).

Summing up, the expression (5) with Eqs. (8) and (9) for effective heat conductivity k_{eff} includes the expression derived in Refs. 8 and 9 as a special case and extends it by considering both diffuse and specular phonon interactions on the matrix-particle interface. In Sec. II C, we shall compare predictions of both formulas with results of observations. One advantage of Eq. (5) with Eqs. (8) and (9) we can already see at this point. In the limit $\phi \to 1$ (i.e., in the absence of the matrix), our general formula gives the correct heat conductivity, namely the heat conductivity k_p of particles. This is not the case for the formula (with $\alpha \neq 0$) derived in Refs. 8 and 9 (see also Fig. 1).

C. Comparison with results of Monte Carlo simulations and experimental observations

We illustrate the expression (5) on SiGe nanocomposite with Si nanoparticles dispersed in a Ge matrix. The material parameters used in calculation are presented in Table I. This nanocomposite has also been previously simulated by Monte Carlo method.[22] Fig. 1 compares our results with the Minnich-Chen[8] formula and with Monte Carlo simulations for $a_p = 5$, 25, 100 nm. The curves corresponding to $0 < s < 1$ lie between the curves corresponding to $s = 0$ and $s = 1$. We see that in the case $s = 1$ (i.e., for pure specular reflection) the predictions implied by Eqs. (5) and (8) differ substantially from the Monte Carlo simulations. On the other hand, in the case of pure diffuse scattering (i.e., when $s = 0$) we see an agreement for all volume fractions. A significant difference between the specular and diffuse effective thermal conductivities is observed in particular in higher volume fractions. It is worthwhile to remark that our results (except the in the case when $s = 1$) are similar to those implied by the Minnich and Chen formula for smaller particle volume fractions. For all particle sizes and in the case of pure diffuse scattering (i.e., $s = 0$), the formulas (5) and (8) predict higher values than does the Minnich-Chen formulas. Moreover, as we have already noted, the effective heat conductivity calculated from Eqs. (5) and (8) approaches the effective thermal conductivity k_p of dispersed nanoparticles when $\phi \to 1$. This difference between our results and the Minnich-Chen formulas becomes more pronounced when the particle radius increases. A difference is also seen for smaller particle sizes in moderate volume fractions. By choosing an appropriate value for s (in other words, choosing an appropriate combination of specular and diffuse scattering), we are able to bring predictions implied by Eqs. (5) and (8) closer to results of Monte Carlo simulation for all particle sizes. Our results also indicate how the effective thermal conductivity of the nanocomposite would change if the particle-matrix surfaces were modified (for example, lowering the temperature to a few Kelvin or changing the roughness of the nanoparticle) to favor specular reflections.

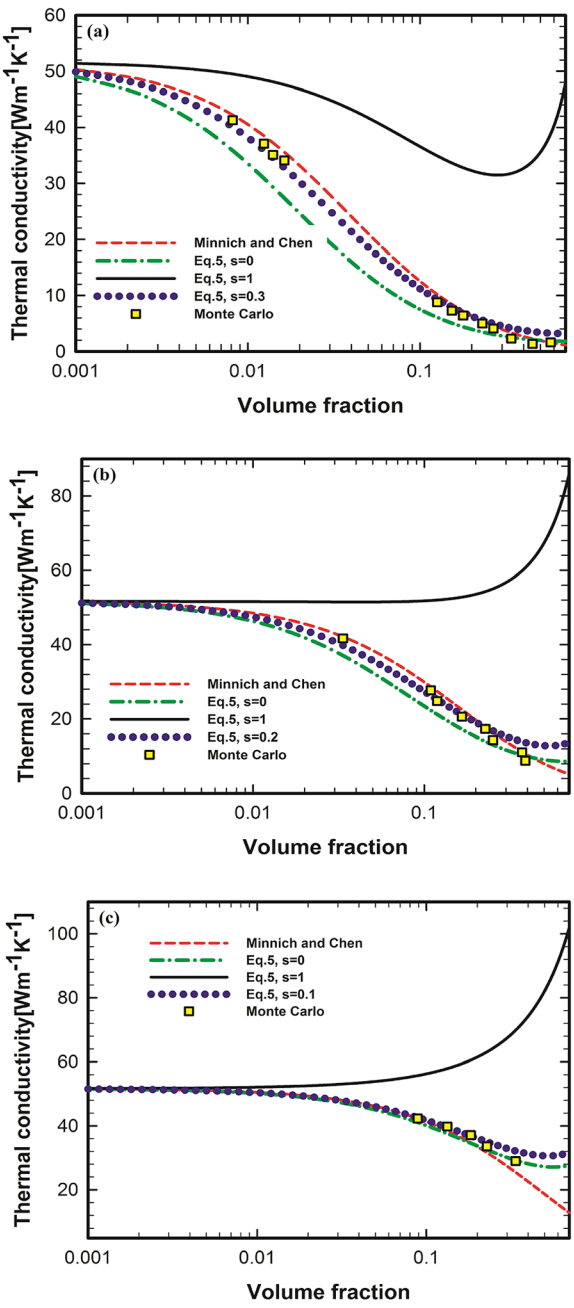

FIG. 1. Effective thermal conductivity of a SiGe nanocomposite comprising spherical Si particles with the radius: (a) $a_p = 5$ nm, (b) $a_p = 25$ nm, and (c) $a_p = 100$ nm as a function of the particle volume fraction ϕ.

Finally, our results are compared with the experimental data[26] for the effective thermal conductivity of nanocomposites with silicon dioxide (SiO_2) and aluminium nitride (AlN) particles embedded in epoxy matrix. The material parameters required for calculations are presented in Table I. Fig. 2 depicts the nanocomposite with SiO_2 particles. Our predictions appear to be in a very good agreement with the experimental data. This is not, however, the case for the nanocomposite with AlN particles. This maybe due to the fact that our model assumes spherical particles of the same size and AlN nanoparticles are not spherical and nor their size distribution is wide. On the other hand, the SiO_2 nanoparticles are spherical and they have a narrow size distribution.

Summing up, our results confirm the anticipated conclusion that the more obstacles the phonons encounter (in

TABLE I. Material parameters used in calculations.

Material	C ($\times 10^6$Jm^{-3}K^{-1})	v (ms^{-1})	Λ_b (nm)	ρ (kg m^{-3})
Si	0.93[a]	1804[a]	268[a]	2330[a]
Ge	0.87[a]	1042[a]	171[a]	5330[a]
SiO_2	1.687[b]	4400[b]	0.558[b]	2278[b]
AlN	2.7[c]	6972[c]	51[d]	3300[c]
Epoxy	1.91[e]	2400[e]	0.11[f]	1970[e]

[a]Reference 18.
[b]Reference 23.
[c]Reference 24.
[d]Calculated from $\Lambda_b = 3k/Cv$ by considering $k = 320$ Wm^{-1}K^{-1} from Ref. 24.
[e]Reference 25.
[f]Calculated from $\Lambda_b = 3k/Cv$ by considering $k = 0.168$ Wm^{-1}K^{-1} from Ref. 26.

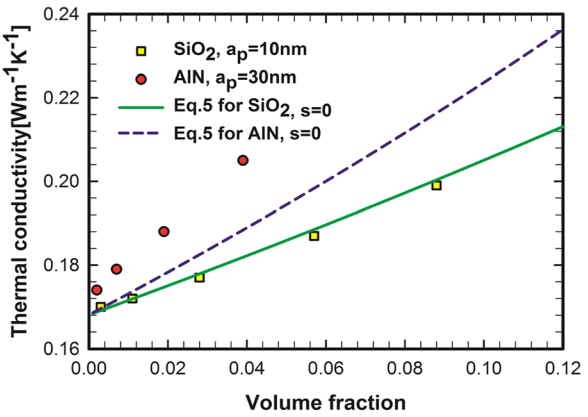

FIG. 2. Experimental and calculated values of the effective thermal conductivity as a function of the volume fractions ϕ of SiO_2 and AlN embedded in epoxy resin.

particular the larger is the particle-matrix interface and the more diffuse is the scattering on it) the lower is the thermal conductivity. We also see that the phonon interactions on the matrix-particle interface are predominantly diffuse (due to the complexity of the interface). We emphasize that the latter conclusion appears in our investigation as a result of the comparison of predictions with experimental observations and not as an initial assumption.

III. TEMPERATURE DEPENDENCE of k_{eff}

The transformation that we have made in Sec. II, namely the transformation from Eq. (1) to Eq. (8), provides also the dependence of k_{eff} on the temperature T. We have lost it in the previous section in the approximation made in the second equality in Eq. (2). The temperature dependence of k enters in Eq. (2) as a parameter in the dependence of C, v, and Λ on ω. We shall now repeat the calculations made in Sec. II B but without the approximation. We restrict ourselves in this section to diffuse scattering (i.e., we put $s=0$ in Eq. (5)) since as we have seen in Sec. II C, the diffuse scatterings on the matrix-particle boundary play a dominant role. In order to deduce from Eq. (2) the temperature dependence, we need the functions $C(T,\omega), v(T,\omega), \Lambda^{(d)}_{b,i}(T,\omega), \Lambda^{(d)}_{coll,i}(T,\omega)$, and $\Lambda^{(d)}_{TBR,i}(T,\omega)$, $i=p,\ m$. They all are well known in the Boltzmann-Peierls theory of phonon propagation.

Following Refs. 21, 27, and 28, we use Debye approximation, take the phonon group velocity v to be a constant independent of ω and T, and the volumetric specific heat per unit frequency at the frequency ω, $C(T,\omega)$, given by

$$C(T,\omega)=\frac{3\hbar^2}{2\pi^2 v_i^3 k_B T^2}\frac{w^4\exp(\hbar\omega/k_BT)}{[\exp(\hbar\omega/k_BT)-1]^2}\qquad i=m,p, \quad (10)$$

where $\hbar$ is the reduced Planck's constant, k_B is the Boltzmann constant. The limits of integration in Eq. (2) are 0 and ω_D that is the Debye frequency cutoff.

Next, we turn to the phonon mean free paths. As for the collision contribution, we see that both $\Lambda^{(d)}_{coll,m}$ and $\Lambda^{(d)}_{coll,p}$ are independent of ω and T. As for the $\Lambda^{(d)}_{b,m}$ and $\Lambda^{(d)}_{b,p}$, we use the expression $\frac{1}{\Lambda^{(d)}_{b,i}}=B_iT\omega^2\exp(-\frac{\theta_i}{T})$; $i=m,p$. B and θ are constant parameters determined by fitting experimental data.[28]

Finally, we address $\Lambda^{(d)}_{TBR,m}$ and $\Lambda^{(d)}_{TBR,p}$. We use the expressions given in Eq. (7) with

$$t^{(d)}_{jl}=\frac{\dfrac{3\hbar^2}{2\pi^2 v_l^2 k_B T^2}\displaystyle\int_0^{\omega_{D,l}}\frac{\omega^4\exp(\hbar\omega/k_BT)}{[\exp(\hbar\omega/k_BT)-1]^2}d\omega}{\dfrac{3\hbar^2}{2\pi^2 v_l^2 k_B T^2}\displaystyle\int_0^{\omega_{D,l}}\frac{w^4\exp(\hbar\omega/k_BT)}{[\exp(\hbar\omega/k_BT)-1]^2}d\omega+\dfrac{3\hbar^2}{2\pi^2 v_j^2 k_B T^2}\displaystyle\int_0^{\omega_{D,j}}\frac{\omega^4\exp(\hbar\omega/k_BT)}{[\exp(\hbar\omega/k_BT)-1]^2}d\omega},\quad j,l=p,m;\ j\neq l. \quad (11)$$

We have now all what we need to evaluate the effective heat conductivity coefficient k_{eff} given in Eq. (8). We shall make the evaluation explicitly for the dispersion of Si particles in Ge discussed already in Sec. II C. We need the parameters B and θ, appearing in bulk mean free path expression, for both Si and Ge. We find them by fitting the experimental data reported in Ref. 29. For Si, we obtain $B=5.753\times10^{-23}\,s^2m^{-1}K^{-1}$ and $\theta=199.2\,K$ and we expect the best fit coefficients for the Ge as $B=1.655\times10^{-22}\,s^2m^{-1}K^{-1}$ and $\theta=78.92\,K$. Fig. 3 shows how well the bulk thermal conductivity model fits the experimental data for both silicon and germanium. The Debye frequency cutoff of Si and Ge are $9.12\times10^13s^{-1}$ and $5.14\times10^13s^{-1}$,[30] respectively, and the phonon group velocities for Si and Ge 6400 m/s and 3900 m/s.[18] Fig. 4 shows the thermal conductivity of SiGe nanocomposites as a function of volume fraction of silicon for different temperatures and different silicon particle sizes. The thermal conductivity decreases from $72\,Wm^{-1}K^{-1}$ at $\phi=1\%$ to $26\,Wm^{-1}K^{-1}$ at $\phi=20\%$ for 200 K, while there is almost no difference in the thermal conductivity of the nanocomposite ($14\,Wm^{-1}K^{-1}$ at $\phi=1\%$ to $10\,Wm^{-1}K^{-1}$ at $\phi=20\%$) at high temperatures around 1000 K. This observation may be explained by the fact that the effect of the interface scattering is more important at lower temperatures, while the Umklapp (internal) scattering has a strong effect at high temperatures.[31] Another argument explaining Fig. 4 is the following: An increase in the temperature causes a reduction in the transmission coefficient from

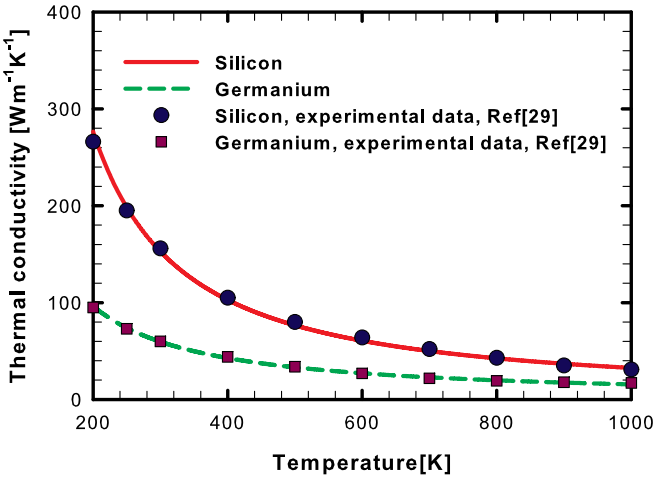

FIG. 3. Temperature dependence of theoretical phonon thermal conductivities for bulk silicon and germanium fitted to experimental data.

matrix to particles. This reduction then increases the thermal boundary resistance, and consequently the thermal conductivity of the dispersion is reduced. Thermal conductivities of nanocomposites calculated for different particle sizes and volume fractions as a function of temperature are plotted in Fig. 5. As shown in Fig. 5(a), the thermal conductivity is significantly reduced with increasing the temperature for all particle sizes at the concentration of 1%. In this condition, due to small amount of nanoparticles, probability of phonon-interface scattering decreases, while, possibility of phonon-phonon (internal) scattering rises. As we expect, the thermal conductivities are the smallest at high temperatures.

At elevated volume fractions and smaller particle sizes, the thermal conductivity of nanocomposites is seen to become almost independent of the temperature (Fig. 5(b) for $a_p = 10\,\text{nm}$). This is due to the dominance of the interface scattering. However, it is remarkable to note that the influence of the internal scattering (phonon-phonon Umklapp scattering) may even become weaker than that of the interface scattering. This happens when nanocomposites have high volume fractions and smaller particle sizes. Despite the insensitivity of the heat conductivity to temperature changes at higher volume fractions and smaller particle sizes, the smallest thermal conductivities are expected to arise precisely in such conditions due to the relative increase in the interface scattering area per unit volume[32] implying strong confinement of phonon transport at the particle matrix interface.

Summing up, we see the heat conductivity decreases with increasing the temperature. Moreover, we see again that the larger are obstacles for phonons (i.e., the larger is the particle-boundary interface) the smaller is the heat conductivity. The difference becomes however significantly smaller for high temperatures.

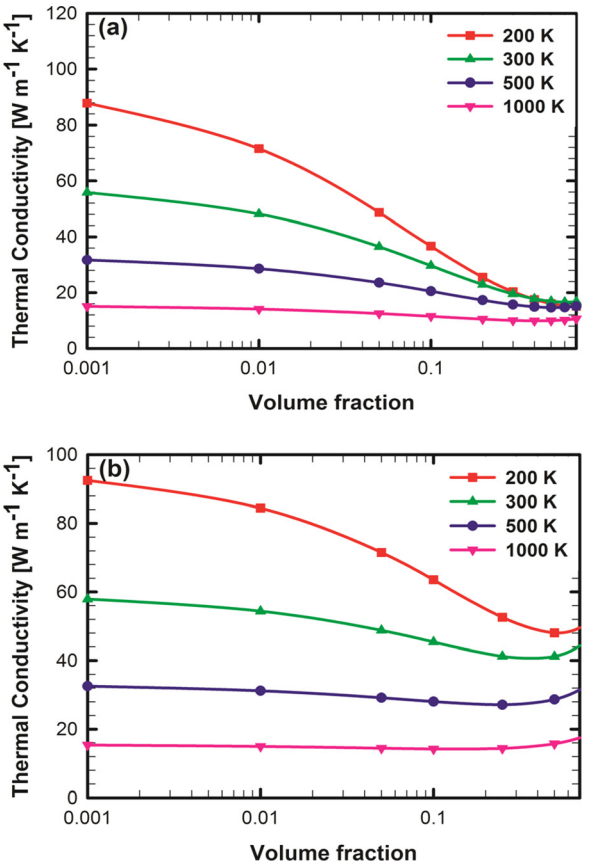

FIG. 4. Effective thermal conductivity of SiGe nanocomposite comprising spherical Si particles with the radius: (a) $a_p = 10\,\text{nm}$, and (b) $a_p = 50\,\text{nm}$ as a function of the particle volume fraction ϕ in different temperatures.

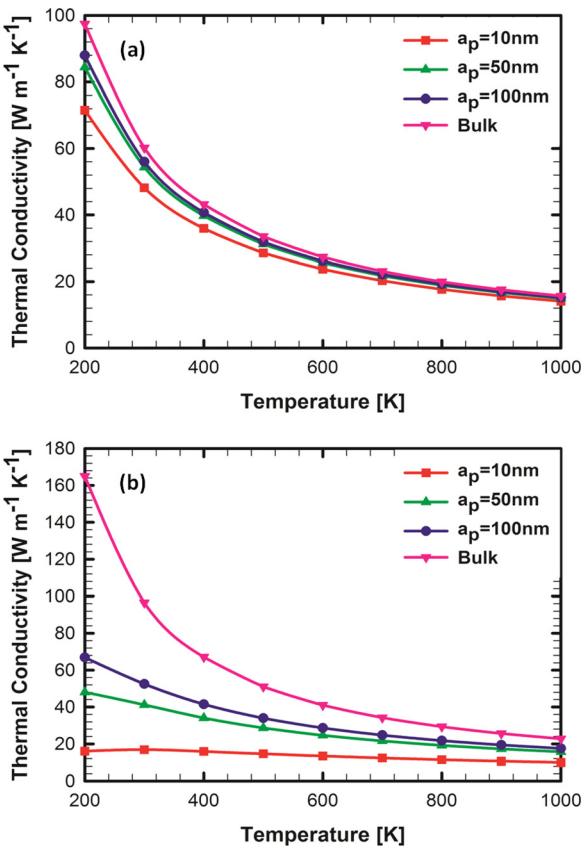

FIG. 5. Effect of temperature on thermal conductivity of Si/Ge nanocomposite for three differences particle sizes and volume fractions (a) $\phi = 0.01$, (b) $\phi = 0.2$, and (c) $\phi = 0.5$.

IV. INFLUENCE OF VARIOUS DEGREES OF AGGLOMERATION on k_{eff}

The distribution of dispersed particles has been so far always uniform (i.e., independent of the spatial coordinate). We now allow the particles to agglomerate. Some of the original particles will form clusters (agglomerates) and the dispersion becomes a dispersion of two types of "particles": the remaining original particles (their number is $N^{(out)}$) and the agglomerates (their number is $N^{(agg)}$). Both the original particles and the agglomerates are assumed to be uniformly distributed (i.e., their distribution is assumed to be independent of the spatial coordinate). If $N^{(in)}$ is the number of the original particles in a single agglomerate and $N^{(p)}$ is the number of the original particles in the dispersion without agglomeration then, $N^{(p)} = N^{(out)} + N^{(in)}N^{(agg)}$, which then implies a similar relation for the volume fractions ϕ

$$\phi^{(p)} = \phi^{(out)} + \phi^{(in)}\phi^{(agg)}, \tag{12}$$

where

$$\begin{aligned} \phi^{(p)} &= \frac{N^{(p)}V^{(p)}}{V}; \quad \phi^{(out)} = \frac{N^{(out)}V^{(p)}}{V}; \\ \phi^{(in)} &= \frac{N^{(in)}V^{(p)}}{V^{(agg)}}; \quad \phi^{(agg)} = \frac{N^{(agg)}V^{(agg)}}{V}, \end{aligned} \tag{13}$$

where V is the total volume of the dispersion, $V^{(p)}$ is the volume of a single original particle, and $V^{(agg)}$ volume of a single agglomerate.

To investigate heat conduction in media with agglomerates, we use the same effective medium approach that we have used in previous sections for media without agglomerates. We apply it now in three steps: (*Step 1*) we homogenize inside a single agglomerate, (*Step 2*) we homogenize outside the agglomerates, and finally (*Step 3*) we homogenize the dispersion of agglomerates. For each step of inhomogeneity, we use the formula (5) derived in Sec. II.

For *Step 1* and *Step 2*, we apply Eq. (5) with related volume fractions $\phi^{(in)}$ and $\phi^{(out)}$, respectively. Note that the specific heat capacity, phonon group velocity and bulk mean free path of the matrix, and the dispersed particles in *Step 1* and *Step 2* are presented in Table I; also the size of dispersed particles for these steps is the same and equal to the size of the original particles in the dispersion without agglomeration. After performing the first two steps, the equivalent bulk thermal conductivities of the matrix and dispersed particles are determined. It means that we have now a heterogeneous media consisting an equivalent bulk matrix phase resulted from *Step 2* and an equivalent bulk dispersed phase (agglomerates) resulted from *Step 1*. In *Step 3*, we need the specific heat capacities C_m, C_p, and the phonon group velocities v_m, v_p. We calculate them by using the mixing rule (i.e., $C_m^{(agg)} = C_m^{(out)}(1-\phi^{(out)}) + C_p^{(out)}\phi^{(out)}$ and similarly for C_p, v_m, v_p). The mean free paths of the matrix and agglomerates are calculated by using Eq. (2). Eventually, we use Eqs. (5) and (8) to determine the effective thermal conductivity of the dispersion. The particle size in *Step 3* is the size of the agglomerate.

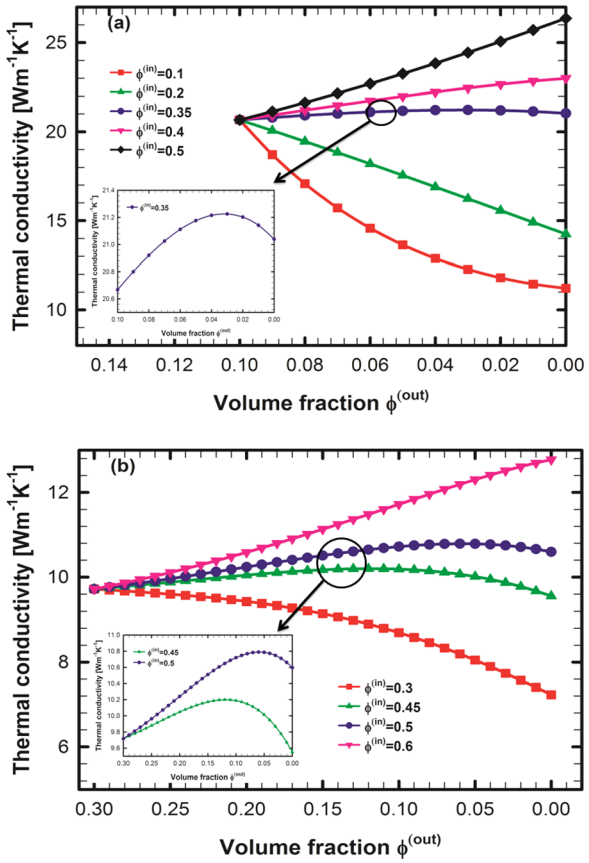

FIG. 6. Effect of agglomeration: (a) $\phi^{(p)} = 0.1$ and (b) $\phi^{(p)} = 0.3$ as a function of the volume fraction of well-dispersed particles, $\phi^{(out)}$ for different degree of agglomeration.

Figs. 6(a) and 6(b) illustrate the evolution of thermal conductivity of dispersion with $\phi^{(in)}$. As a case study, we look at the thermal conductivity of SiGe dispersion. The material parameters used in this calculation have been already presented in Table I. The radius of the original particles is 20 nm and the gyration radius of the agglomerates is assumed 5 times the radius of original particles. The x-axis is the volume fraction $\phi^{(out)}$ of the original particles outside agglomerates. Passing from left to right is thus passing from low to higher degrees of agglomeration.

The matrix-agglomerate scattering is assumed to be purely diffuse. This is because we expect the matrix-agglomerate interface to be, in general, rougher than the particle-matrix interface. In Figs. 6(a) and 6(b), we also assume that the matrix-particle scattering is purely diffuse. The effect of specularity in the particle-matrix scattering leads to an increase in the thermal conductivity.

Results show that agglomeration can either decrease or increase the thermal conductivity. The increase occurs for compact agglomerates (i.e., for large $\phi^{(in)}$) and decrease for agglomerates that are less compact. For intermediate degrees of compactness of the agglomerates (i.e., intermediate values of $\phi^{(in)}$) the heat conductivity first increases with increasing the degree of agglomeration (i.e., with decreasing $\phi^{(out)}$) and then, after reaching a certain critical value of the agglomeration, starts to decrease. We believe that the possibility to influence the heat conductivity by nonuniform distribution of

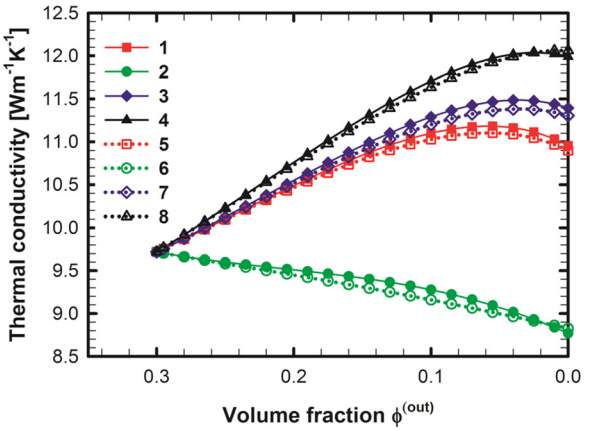

FIG. 7. Effect of different sizes of agglomerates: (1) $a_p = 20\,\text{nm}$, $\phi^{(p)} = 0.3$, $\phi^{(inA)} = 0.35$, $\phi^{(inB)} = 0.4$, $\phi^{(aggA)} = 0.1\phi^{(aggB)}$, $a_p^{(A)} = 60\,\text{nm}$, $a_p^{(B)} = 200\,\text{nm}$; (2) the same as in (1) except that $\phi^{(aggA)} = 1.5\phi^{(aggB)}$; (3) and (4) the same as in (1) except that $\phi^{(inA)} = 0.5$ for (3) and $a_p^{(B)} = 300\,\text{nm}$ for (4). The homogenization in ((1)–(4)) is (AB) and in ((5)–(8)) (BA).

particles may be of particular importance for optimizing efficiency of thermoelectric devices.

In applications, the agglomerates are, of course, not necessarily all identical. In order to illustrate this more general case, we consider two types of agglomerates denoted "A" and "B." The relation (12) becomes $\phi^{(p)} = \phi^{(out)} + \phi^{(inA)}\phi^{(aggA)} + \phi^{(inB)}\phi^{(aggB)}$ (we use a notation that extends in a natural way the notation used in Eq. (12)). In the process of homogenization, we now have two possibilities: *(homogenization AB)* After making the three homogenizations "outside," "inside A," and "inside B," we continue to homogenize "outside" with agglomerates "A" and then homogenize the result with agglomerates "B." (*homogenization BA*) We do the last two homogenizations in reverse order (i.e., we homogenize "outside" with agglomerates "B" and then homogenize the result with agglomerates "A." Results for one particular choice of agglomerates are depicted in Fig. 7. We see that nonuniformity in the sizes of agglomerates does not change significantly the effect seen in the previous figures. We can also see that the order of the homogenization has a very small effect on final results.

V. CONCLUDING REMARKS

We have used the well known combination of the effective medium approach and the phonon approach to study heat conduction in heterogeneous media composed of a homogeneous matrix in which spherical particles are dispersed. In particular, we have investigated how the effective heat conductivity coefficient k_{eff} of the composite is influenced by the type of phonon scattering on the particle-matrix interface, by changes in the temperature, and by various degrees of agglomeration of the dispersed particles. The influence of the interface enters the analysis in the thermal boundary resistance phonon mean free path. The temperature dependence, implicitly appearing in the frequency dependencies of all the phonon-related quantities entering the formula for k_{eff}, is made explicit with the assistance of computers. In the investigation of the influence of agglomeration, we apply homogenization separately to the medium inside the agglomerate, outside the agglomerates, and finally to the dispersion of agglomerates.

Our results show that the more obstacles the phonons encounter in the composites the lower is the thermal conductivity. The main obstacle is the particle-matrix interface. Given the volume fraction of the particles, the particle-matrix interface can be increased by decreasing the size of the particles and increasing their number. We also show that the more diffuse is the phonon-interface scattering the lower is the thermal conductivity. By comparing our predictions with results of experimental observations we have seen that the diffuse scattering is dominant but a small amount of the specular scattering is needed to improve the fit.

As for the temperature dependence, we see the decrease of the heat conductivity with increasing the temperature. Moreover, we also see that the differences caused by changes in the size of the particle-matrix interface and the type of phonon-particle scattering, become considerably smaller for higher temperatures.

Particularly interesting results arise in the study of the influence of the agglomeration on the effective heat conductivity coefficient k_{eff}. Our investigation shows that both decrease and increase of k_{eff} can be achieved. The increase occurs in general for compact agglomerates and the decrease for agglomerates that are only slightly more compact than the initial nonagglomerated composite. We do not investigate in this paper the influence of the agglomeration on the electric heat conductivity coefficient. In a future paper, we intend to explore the potential of agglomeration as a tool to increase the efficiency of thermoelectric devices.

ACKNOWLEDGMENTS

This article was partially supported by Natural Sciences and Engineering Research Council of Canada.

[1]D. P. H. Hasselman and L. F. Johnson, J. Compos. Mater. **21**, 508 (1987).
[2]C.-W. Nan, R. Birringer, D. R. Clarke, and H. Gleiter, J. Appl. Phys. **81**, 6692 (1997).
[3]J. C. Maxwell, *Treatise on Electricity and Magnetism*, 2nd ed. (Clarendon, Oxford, 1881).
[4]R. Peierls, Ann. Phys. **395**, 1055 (1929).
[5]J. A. Reissland, *The Physics of Phonons* (John Willey and Sons, London, 1973).
[6]W. Dreyer and H. Struchtrup, Continuum Mech. Thermodyn. **5**, 3 (1993).
[7]M. Grmela, G. Lebon, and C. Dubois, Phys. Rev E **83**, 061134 (2011).
[8]A. J. Minnich and G. Chen, Appl. Phys. Lett. **91**, 073105 (2007).
[9]J. Ordonez-Miranda, R. Yang, and J. J. Alvarado-Gil, Appl. Phys. Lett. **98**, 233111 (2011).
[10]M. S. Dresselhaus, G. Chen, M. Y. Tang, R. G. Yang, H. Lee, D. Z. Wang, Z. F. Ren, J. P. Fleurial, and P. Gogna, Adv. Mater. **19**, 1043 (2007).
[11]A. Minnich, M. S. Dresselhaus, Z. F. Ren, and G. Chen, Energy Environ. Sci. **2**, 466 (2009).
[12]K. F. Hsu, S. Loo, F. Guo, W. Chen, J. S. Dyck, C. Uher, T. Hogan, E. K. Polychroniadis, and M. G. Kanatzidis, Science **303**, 818 (2004).
[13]G. H. Zhu, H. Lee, Y. C. Lan, X. W. Wang, G. Joshi, D. Z. Wang, J. Yang, D. Vashaee, H. Guilbert, A. Pillitteri, M. S. Dresselhaus, G. Chen, and Z. F. Ren, Phys. Rev. Lett. **102**, 196803 (2009).
[14]B. Poudel, Q. Hao, Y. Ma, Y. Lan, A. Minnich, B. Yu, X. Yan, D. Wang, A. Muto, D. Vashaee, X. Chen, J. Liu, M. S. Dresselhaus, G. Chen, and Z. F. Ren, Science **320**, 634 (2008).
[15]A. I. Boukai, Y. Bunimovich, J. Tahir-Kheli, J. K. Yu, W. A. Goddard III, and J. R. Heath, Nature **451**, 168 (2008).

[16]X. W. Wang, H. Lee, Y. C. Lan, G. H. Zhu, G. Joshi, D. Z. Wang, J. Yang, A. J. Muto, M. Y. Tang, J. Klatsky, S. Song, M. S. Dresselhaus, G. Chen, and Z. F. Ren, Appl. Phys. Lett. **93**, 193121 (2008).
[17]G. Joshi, H. Lee, Y. Lan, X. Wang, G. Zhu, D. Wang, R. W. Gould, D. C. Cuff, M. Y. Tang, M. S. Dresselhaus, G. Chen, and Z. F. Ren, Nano Lett. **8**, 4670 (2008).
[18]G. Chen, Phys. Rev. B **57**, 14958 (1998).
[19]G. Chen, J. Heat Transfer **118**, 539 (1996).
[20]C. Dames and G. Chen, J. Appl. Phys. **95**, 682 (2004).
[21]G. Chen, *Nanoscale Energy Transport and Conversion: A Parallel Treatment of Electrons, Molecules, Phonons, and Photons: A Parallel Treatment of Electrons, Molecules, Phonons, and Photons* (Oxford University Press, Oxford, New York, 2005).
[22]M.-S. Jeng, R. Yang, D. Song, and G. Chen, J. Heat Transfer **130**, 042410 (2008).
[23]T. Zeng and G. Chen, J. Heat Transfer **123**, 340 (2001).
[24]Y. Zhao, C. Zhu, S. Wang, J. Z. Tian, D. J. Yang, C. K. Chen, H. Cheng, and P. Hing, J. Appl. Phys. **96**, 4563 (2004).
[25]H. M. Duong, N. Yamamoto, K. Bui, D. V. Papavassiliou, S. Maruyama, and B. L. Wardle, J. Phys. Chem. C **114**, 8851 (2010).
[26]R. Kochetov, A. V. Korobko, T. Andritsch, P. H. F. Morshuis, S. J. Picken, and J. J. Smit, J. Phys. D: Appl. Phys. **44**, 395401 (2011).
[27]J. Callaway, J. Phys. Rev. **113**, 1046 (1959).
[28]N. Mingo, L. Yang, D. Li, and A. Majumdar, Nano Lett. **3**, 1713 (2003).
[29]C. J. Glassbrenner and G. A. Slack, Phys. Rev. **134**, A1058 (1964).
[30]K. Kádas, L. Vitos, and R. Ahuja, Appl. Phys. Lett. **92**, 052505 (2008).
[31]Q. Hao, G. Zhu, G. Joshi, X. Wang, A. Minnich, Z. Ren, and G. Chen, Appl. Phys. Lett. **97**, 063109 (2010).
[32]R. Yang, G. Chen, and M. S. Dresselhaus, Phys. Rev. B **72**, 125418 (2005).